9-4-2017

Synthesis of Non-uniformly Correlated Partially Coherent Sources Using a Deformable Mirror

Milo W. Hyde IV
Air Force Institute of Technology

Santasri Bose-Pillai
Air Force Institute of Technology

R. A. Wood

Synthesis of non-uniformly correlated partially coherent sources using a deformable mirror

Cite as: Appl. Phys. Lett. **111**, 101106 (2017); https://doi.org/10.1063/1.4994669
Submitted: 06 July 2017 . Accepted: 27 August 2017 . Published Online: 07 September 2017

M. W. Hyde, S. R. Bose-Pillai, and R. A. Wood

Synthesis of non-uniformly correlated partially coherent sources using a deformable mirror

M. W. Hyde IV,[1,a)] S. R. Bose-Pillai,[2,b)] and R. A. Wood[1,c)]
[1]*Department of Electrical and Computer Engineering, Air Force Institute of Technology, Dayton, Ohio 45433, USA*
[2]*Department of Engineering Physics, Air Force Institute of Technology, Dayton, Ohio 45433, USA*

(Received 6 July 2017; accepted 27 August 2017; published online 7 September 2017)

The near real-time synthesis of a non-uniformly correlated partially coherent source using a low- actuator-count deformable mirror is demonstrated. The statistical optics theory underpinning the synthesis method is reviewed. The experimental results of a non-uniformly correlated source are presented and compared to theoretical predictions. A discussion on how deformable mirror characteristics such as actuator count and pitch affect source generation is also included.

[http://dx.doi.org/10.1063/1.4994669]

In the past decade, the design and synthesis of partially coherent beams or sources have received much attention. A vast majority of this work has focused on uniformly correlated or Schell-model sources.[1,2] These sources are very easy to synthesize and can be designed to exhibit practically any desired behavior, e.g., self-split,[3] self-steer,[4] rotation,[5] production of needle-like shapes,[6] and generation of rings.[7] The interested reader is referred to Refs. 8–13 for books and reviews on the design, synthesis, and applications of Schell-model sources.

While Schell-model source research remains popular and continues to mature, research into non-uniformly correlated (NUC) sources is burgeoning. These sources can self-focus in the near field and be designed to experience lower scintillation and achieve higher intensity values than the Schell-model and spatially coherent sources when propagating through random media.[14–18] These characteristics make NUC sources potentially useful in applications such as medicine, laser manufacturing, and directed energy.

In contrast to Schell-model sources, NUC sources are harder to synthesize, and only a few papers have been published on this subject: Refs. 19 and 20 are most applicable to computer simulations involving NUC sources. References 21 and 22 present the experimental results of NUC sources; however, both use liquid crystal spatial light modulators (SLMs) to generate NUC source realizations and therefore, because of speed, are not currently suitable for use in the applications listed above.

In this paper, the near real-time synthesis of a NUC source using a low-actuator-count segmented deformable mirror (DM) is demonstrated. The NUC source is physically realized using the analytical approach discussed in Refs. 23 and 24. In the following paragraphs, the relevant theory from Refs. 23 and 24 is briefly reviewed. Next, the experimental results of a NUC source are presented and compared to theoretical predictions. Included with the results are discussions of the experimental setup and the pros and cons of using a DM versus an SLM to synthesize NUC sources.

Here, a variant of the NUC source originally introduced by Lajunen and Saastamoinen (hereafter referred to as an LS source)[14] is physically realized using a DM. The theory presented here is specialized to this source; the general treatment is presented in Refs. 23 and 24.

Let an instance of a random optical field be

$$U(\boldsymbol{\rho}) = \tau(\boldsymbol{\rho})\exp\left(\mathrm{j}\psi|\boldsymbol{\rho}-\boldsymbol{\gamma}|^2\right), \tag{1}$$

where $\mathrm{j}=\sqrt{-1}$, $\boldsymbol{\rho}=\hat{\boldsymbol{x}}x+\hat{\boldsymbol{y}}y$, τ is a complex function, ψ is a random number or weight, and $\boldsymbol{\gamma}=\hat{\boldsymbol{x}}\gamma_x+\hat{\boldsymbol{y}}\gamma_y$ is a real-valued vector.[23] Taking the autocorrelation of Eq. (1) yields

$$W(\boldsymbol{\rho}_1,\boldsymbol{\rho}_2) = \tau(\boldsymbol{\rho}_1)\tau^*(\boldsymbol{\rho}_2) \times \langle \exp[\mathrm{j}(|\boldsymbol{\rho}_1-\boldsymbol{\gamma}|^2-|\boldsymbol{\rho}_2-\boldsymbol{\gamma}|^2)\psi]\rangle, \tag{2}$$

where W is the cross-spectral density function.[1] The moment in Eq. (2) is the characteristic function of the random variable ψ

$$\chi(\boldsymbol{\rho}_1,\boldsymbol{\rho}_2) = \int_{-\infty}^{\infty} \exp\left[\mathrm{j}\left(|\boldsymbol{\rho}_1-\boldsymbol{\gamma}|^2-|\boldsymbol{\rho}_2-\boldsymbol{\gamma}|^2\right)\psi\right] \times P(\psi)\mathrm{d}\psi, \tag{3}$$

where P is the probability density function (PDF).[2] Note that χ is the correlation function of the resulting NUC source, typically denoted by μ in the literature.

The correlation function of an LS source is

$$\mu(\boldsymbol{\rho}_1,\boldsymbol{\rho}_2) = \exp\left[-\frac{\left(|\boldsymbol{\rho}_1-\boldsymbol{\gamma}|^2-|\boldsymbol{\rho}_2-\boldsymbol{\gamma}|^2\right)^2}{2\delta^2}\right], \tag{4}$$

where δ is akin to the spatial correlation radius of traditional uniformly correlated (Schell-model) sources.[14] It is clear

[a)]Electronic mail: milo.hyde@afit.edu
[b)]Electronic mail: santasri.bosepillai@afit.edu
[c)]Also with the John A. Paulson School of Engineering and Applied Sciences, Harvard University, Cambridge, MA 02138, USA. Electronic mail: rwood@college.harvard.edu.

from the near Fourier transform relationship between $\chi = \mu$ and P [recall Eq. (3)] that ψ is a zero-mean, $1/\delta^2$-variance Gaussian random number, i.e.,

$$P(\psi) = \frac{1}{\sqrt{2\pi}(1/\delta)} \exp\left[-\frac{\psi^2}{2(1/\delta)^2}\right]. \tag{5}$$

Thus, a partially coherent source with a μ value given in Eq. (4) can be synthesized by incoherently summing many realizations of Eq. (1), where ψ values are drawn from the PDF in Eq. (5). Since the phase function $|\boldsymbol{\rho} - \boldsymbol{\gamma}|^2$ is essentially defocus (a low-order aberration), these sources can be produced with a small DM—small referring to the number of actuators. This is demonstrated below.

Figure 1 shows a schematic of the experimental setup for realizing NUC sources. Coherent light emitted from a 2 mW 632.8 nm helium-neon (HeNe) laser is expanded 20× before passing through a half-wave plate (HWP) and a linear polarizer (LP). The HWP-LP combination is used to manually control power and to transform the laser's linear polarization state to vertical polarization—the control state of the SLM.

The light is then incident on the SLM, which is used to shape and apply a 60 cm focus to the light beam. The SLM used here is a Meadowlark Optics P512 which has a 512×512 liquid crystal pixel array with a 15 μm pitch. Using a diagonal sawtooth phase ramp or grating,[25–27] the SLM produces the desired field in the first diffraction order; thus, a spatial filter—400 mm lens (L1), iris (I), and 100 mm lens (L2)—is used to block all orders other than the first.

After passing through the spatial filter, the light is incident on the DM located approximately 100 mm beyond L2. The DM is a Boston Micromachines Mini-SLM which is a 32 actuator (6×6 with the corner actuators removed) segmented DM with a 300 μm pitch. Since the DM is approximately four times smaller than the SLM, the spatial filter images the SLM field, at 1/4 size, onto the DM. The DM applies the random defocuses, whose weights are drawn from the PDF in Eq. (5), to the incident field. For ease of alignment, a 50:50 beam splitter (BS) is situated immediately before the DM so that it can be operated at normal incidence.

The light reflected from the DM passes back through the BS and then through a neutral density filter (NDF) to further reduce the power and is finally received by the camera (C) located approximately 40 cm from the DM. The camera used here is a Lumenera Lw135RM which has a 1392×1040 detector array with a 4.65 μm pitch. Recall that in addition to shaping the beam, the SLM applies a 60 cm focus to the light incident on the DM. Thus, the camera measures near-field intensities where NUC sources exhibit interesting behaviors, most notably self-focusing.[14,16,17,22]

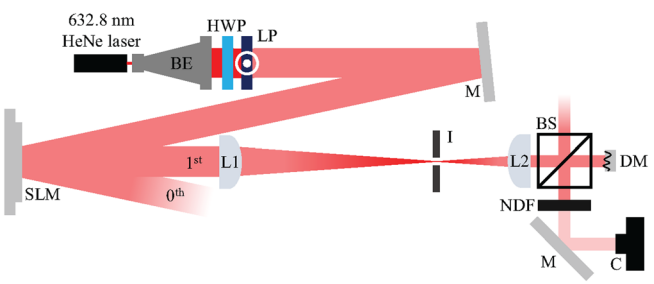

FIG. 1. Schematic of the experimental setup for synthesizing NUC sources. The abbreviations used in the figure are helium neon (HeNe), beam expander (BE), half-wave plate (HWP), linear polarizer (LP), mirror (M), spatial light modulator (SLM), 400 mm lens (L1), iris (I), 100 mm lens (L2), beam splitter (BS), deformable mirror (DM), neutral density filter (NDF), and camera (C).

The LS source generated in this experiment had a cross-spectral density function

$$W(\boldsymbol{\rho}_1, \boldsymbol{\rho}_2) = \mathrm{rect}\left(\frac{x_1}{D_{\mathrm{DM}}}\right)\mathrm{rect}\left(\frac{y_1}{D_{\mathrm{DM}}}\right) \times \mathrm{rect}\left(\frac{x_2}{D_{\mathrm{DM}}}\right)\mathrm{rect}\left(\frac{y_2}{D_{\mathrm{DM}}}\right)\mu(\boldsymbol{\rho}_1, \boldsymbol{\rho}_2), \tag{6}$$

where μ is given in Eq. (4), rect is[28]

$$\mathrm{rect}(x) = \begin{cases} 1 & |x| < 1/2 \\ 1/2 & |x| = 1/2 \\ 0 & \text{otherwise.} \end{cases} \tag{7}$$

$\boldsymbol{\gamma} = -\hat{\boldsymbol{x}}0.6\,\mathrm{mm} - \hat{\boldsymbol{y}}0.6\,\mathrm{mm}$, $D_{\mathrm{DM}} = 1.80\,\mathrm{mm}$, and $\delta = 0.1719$ mm^2. The theoretical spectral density S matching the experimental setup was found by computing

$$S(\boldsymbol{\rho}, z) = \frac{1}{\lambda^2 z^2}\int\int\int\int_{-\infty}^{\infty} W(\boldsymbol{\rho}_1', \boldsymbol{\rho}_2') \times \exp\left[\frac{\mathrm{j}k}{2}\left(\frac{1}{R} + \frac{1}{z}\right)(\rho_1'^2 - \rho_2'^2)\right] \times \exp\left[-\frac{\mathrm{j}k}{z}(\boldsymbol{\rho}_1' - \boldsymbol{\rho}_2') \cdot \boldsymbol{\rho}\right]\mathrm{d}^2\rho_1'\mathrm{d}^2\rho_2', \tag{8}$$

where $\lambda = 632.8\,\mathrm{nm}$, $k = 2\pi/\lambda$, $z = 40\,\mathrm{cm}$, and $R = -60\,\mathrm{cm}$, numerically using fast Fourier transforms. The four-dimensional W was discretized using 180 points per side (approximately 1.05×10^9 points) with a 55.6 μm spacing. The calculation required approximately 129 GB of memory and 410 s to complete on a HP Z820 with two Intel® Xeon® 2.60 GHz processors. The resulting theoretical S was then interpolated to the camera's dimensions for ease of comparison with the experimental results.

The W in Eq. (6) was synthesized in two different experiments. In the first (hereafter referred to as the DM experiment), the DM was used to synthesize μ [Eq. (4)] by applying Gaussian distributed [Eq. (5)] random defocuses to the incident field. The SLM was used to shape the collimated laser field into a flat-topped, square-shaped beam with a 60 cm focus. The phase commands for both devices were of the form

$$\begin{aligned} \Phi_{\mathrm{DM}} &= \arg\left[\exp\left(\mathrm{j}\psi|\boldsymbol{\rho} - \boldsymbol{\gamma}|^2\right)\right] \\ \Phi_{\mathrm{SLM}} &= \arg\left(\exp\left\{\mathrm{j}\left[2\pi\boldsymbol{G}(\boldsymbol{\rho}) \cdot \boldsymbol{\rho} + \frac{k}{2R}\rho^2\right]\right\}\right), \end{aligned} \tag{9}$$

where $\boldsymbol{G}$ was the gradient of the sawtooth grating. Here,

$$\boldsymbol{G}(\boldsymbol{\rho}) = \begin{cases} \hat{\boldsymbol{x}}1/8 + \hat{\boldsymbol{y}}1/8 & \boldsymbol{\rho} \in A \\ 0 & \text{otherwise,} \end{cases} \tag{10}$$

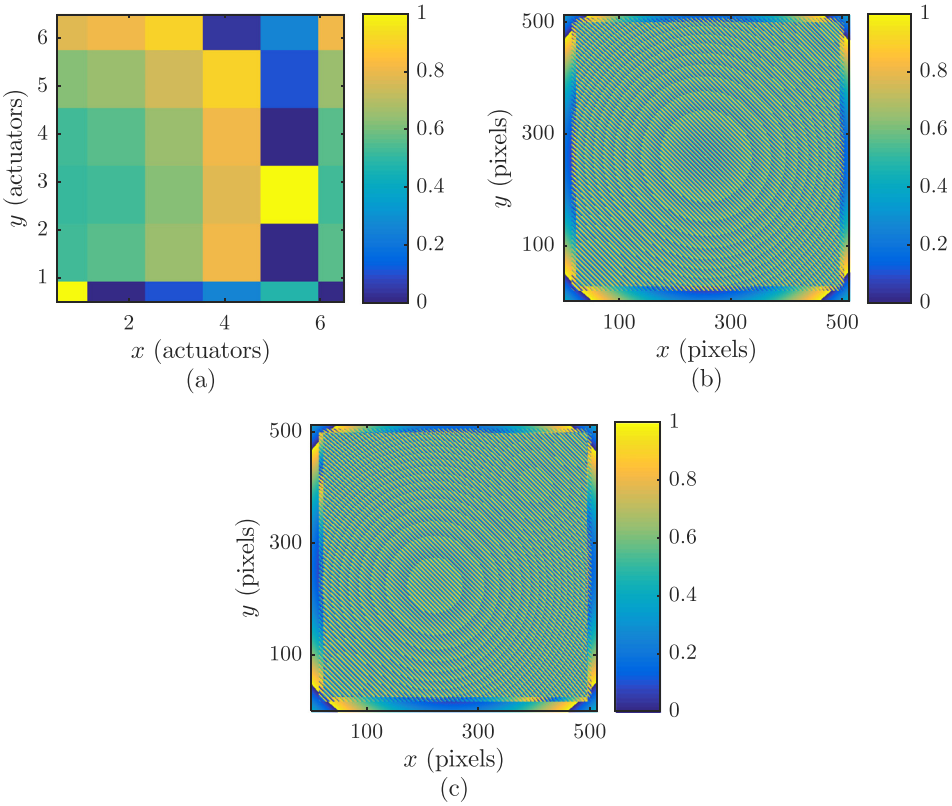

FIG. 2. Example DM Φ_{DM} and SLM Φ_{SLM} commands—(a) example Φ_{DM} from the DM experiment, (b) static Φ_{SLM} from the DM experiment, and (c) example Φ_{SLM} from the SLM experiment. The phase commands in (a), (b), and (c) are in waves.

where A was the area within the rectangle functions in Eq. (6) and $\boldsymbol{G}$ was in waves per pixel.

In the second experiment (called the SLM experiment), the DM surface was held flat and the SLM was used to generate LS field instances. The phase command for the SLM was

$$\Phi_{\mathrm{SLM}} = \arg\left(\exp\left\{\mathrm{j}\left[2\pi \boldsymbol{G}(\boldsymbol{\rho})\cdot\boldsymbol{\rho} + \frac{k}{2R}\rho^2 + \psi|\boldsymbol{\rho}-\boldsymbol{\gamma}|^2\right]\right\}\right). \tag{11}$$

Figures 2(a) and 2(b) show an example Φ_{DM} and the static Φ_{SLM} used in the DM experiment, respectively; Fig. 2(c) shows an example Φ_{SLM} used in the SLM experiment.

In both experiments, the camera continuously collected 66 ms exposures (the max integration time) for approximately 100 s. At that time, the DM, operating at approximately 3 kHz, cycled through 300 000 defocus screens, whereas the SLM, operating at approximately 20 Hz, managed only 2500 defocus screens. The DM and SLM

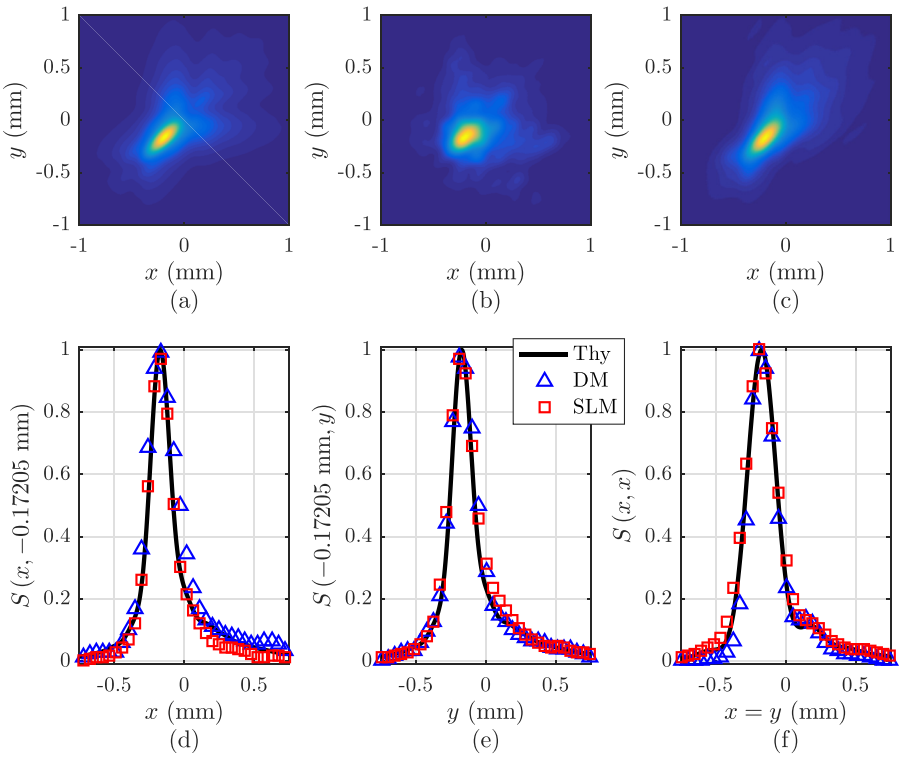

FIG. 3. LS source experimental results—(a) theoretical S, (b) DM S, (c) SLM S, (d) $y = -0.17205$ mm and x slices for the theoretical, DM, and SLM S, (e) $x = -0.17205$ mm and y slices for the theoretical, DM, and SLM S, and (f) $x = y$ slices for the theoretical, DM, and SLM S.

experimental S were then centered for ease of comparison with the theoretical S in Eq. (8).

Figure 3 shows the following results: (a) the theoretical spectral density S, (b) the DM experimental S, (c) the SLM experimental S, (d) $y = -0.17205$ mm (y coordinate of max S) and x slices for the theoretical (solid black trace), DM (blue triangles), and SLM (red squares) S, (e) $x = -0.17205$ mm (x coordinate of max S) and y spectral density slices, and (f) the diagonal, $x = y$ spectral density slices.

Overall, the SLM appears to produce a higher quality S than the DM; both the DM and SLM S are well comparable with theory in the vicinity of the S maximum. These results motivate discussing some of the pros and cons of using a DM to synthesize NUC sources as opposed to an SLM. The main advantage of using a DM over an SLM is speed. The difference in speed between the two devices is quite noticeable in the attached movie (Figure 4 shows the second frame of that movie), which shows the first 100 frames of the data collects. The upper panels [(a) and (b)] show the 66 ms camera images for the DM and SLM, respectively; the lower panels [(c) and (d)] show the running averages. Comparing the DM images appearing in (a) with either (c) or Fig. 3(b), it is clear that the DM operates quick enough such that the spectral density S is produced in a single 66 ms exposure. This is clearly not the case for the SLM. It should be noted that with the proper hardware (which is commercially available), the DM used here can operate even faster—the maximum advertised frame rate is 20 kHz.

While DMs are generally orders of magnitude faster, they typically possess far fewer pixels or actuators than SLMs. This fundamentally limits the "aberrations," including their weights, which can be applied to the wavefront. For instance, here a 6×6 segmented DM with a 300 μm pitch was used to apply a random defocus $\exp(j\psi\rho^2)$, ignoring γ, to the field. The maximum weight ψ that this DM can produce without aliasing the resulting phase is determined by

$$\Delta_{\mathrm{DM}} \left| \frac{\partial \phi}{\partial x} \right|_{\max} \leq \pi, \tag{12}$$

where $\phi = \psi\rho^2$ and $\Delta_{\mathrm{DM}} = 300\,\mu$m is the DM pitch.[29–31] Evaluating the derivative and solving for ψ yield

$$\psi \leq \frac{\pi}{2\Delta_{\mathrm{DM}}|x_{\max}|} = \frac{\pi}{\Delta_{\mathrm{DM}} D_{\mathrm{DM}}} \approx 5.82\,\mathrm{mm}^{-2}. \tag{13}$$

Recalling the PDF given in Eq. (5), this max ψ can be converted into a minimum δ: $\delta \geq 1/\max(\psi) \approx 0.1719\,\mathrm{mm}^2$, which is the δ of the LS source generated above. Any LS source with a δ value less than this cannot be synthesized with this DM. In contrast, the minimum δ that can be synthesized with the SLM is $\delta \geq \Delta_{\mathrm{SLM}} D_{\mathrm{SLM}}/\pi \approx 0.0023\,\mathrm{mm}^2$—recall that the SLM is demagnified by a factor of four in the

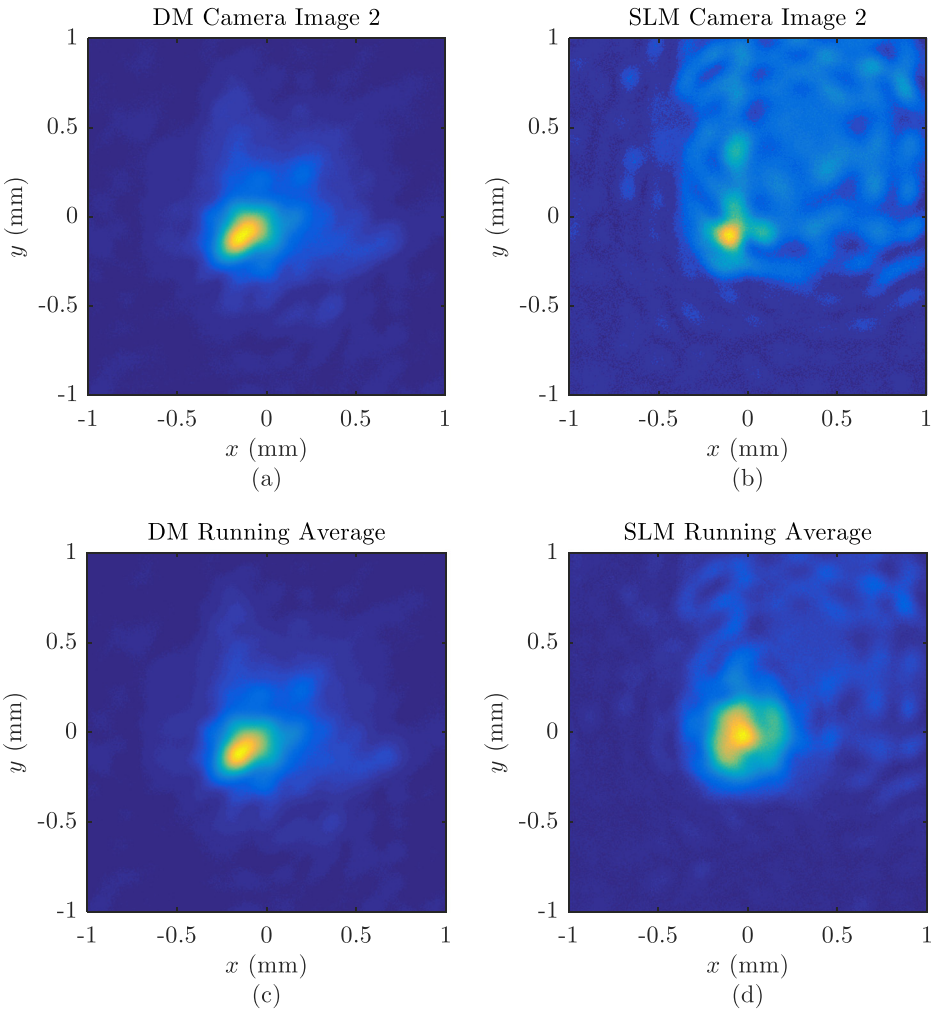

FIG. 4. Second frame of LS source visualization—(a) 66 ms DM frame, (b) 66 ms SLM frame, (c) running average of (a), and (d) running average of (b). (Multimedia view) [URL: http://dx.doi.org/10.1063/1.4994669.1]

experimental setup. This likely explains why the SLM results are qualitatively better than the DM results.

It must be stated that the above analysis applies to wavefront-shaping devices where the phase is applied, modulo 2π. For devices such as continuous face-sheet DMs, other factors—most importantly actuator stroke and, to a lesser degree, interactuator coupling—combine, resulting in a minimum δ that can be accurately synthesized with that device.

In conclusion, the near real-time synthesis of a NUC source using a low-actuator-count segmented DM was demonstrated. The theory underpinning the approach was briefly reviewed. The experimental results of a NUC source were presented and found to be in very good agreement with theoretical predictions. Finally, the pros and cons of using a DM, as opposed to an SLM, to synthesize NUC sources were discussed.

With faster DM hardware, which is commercially available, the approach and physical setup discussed in this paper can be used to synthesize NUC sources in real time for applications such as directed energy, laser manufacturing, particle manipulation, and medicine.

The views expressed in this paper are those of the authors and do not reflect the official policy or position of the U.S. Air Force, the Department of Defense, or the U.S. Government.

[1]L. Mandel and E. Wolf, *Optical Coherence and Quantum Optics* (Cambridge University, 1995).
[2]J. W. Goodman, *Statistical Optics*, 2nd ed. (Wiley, 2015).
[3]Y. Chen, J. Gu, F. Wang, and Y. Cai, Phys. Rev. A **91**, 013823 (2015).
[4]Y. Chen, S. A. Ponomarenko, and Y. Cai, Sci. Rep. **7**, 39957 (2017).
[5]Z. Mei and O. Korotkova, Opt. Lett. **42**, 255 (2017).
[6]J. Li, F. Wang, and O. Korotkova, Opt. Express **24**, 17779 (2016).
[7]Z. Mei and O. Korotkova, Opt. Lett. **38**, 91 (2013).
[8]O. Korotkova, *Random Light Beams: Theory and Applications* (CRC Press, 2014).
[9]Y. Cai, Y. Chen, and F. Wang, J. Opt. Soc. Am. A **31**, 2083 (2014).
[10]Y. Cai, Y. Chen, J. Yu, X. Liu, and L. Liu, in *Progress in Optics*, edited by T. D. Visser (Elsevier, 2017), Vol. 62, Chap. 3, pp. 157–223.
[11]G. Gbur and T. Visser, in *Progress in Optics*, edited by E. Wolf (Elsevier, 2010), Vol. 55, Chap. 5, pp. 285–341.
[12]G. Gbur, J. Opt. Soc. Am. A **31**, 2038 (2014).
[13]*Vectorial Optical Fields: Fundamentals and Applications*, edited by Q. Zhan (World Scientific, 2014).
[14]H. Lajunen and T. Saastamoinen, Opt. Lett. **36**, 4104 (2011).
[15]M. Santarsiero, R. Martínez-Herrero, D. Maluenda, J. C. G. de Sande, G. Piquero, and F. Gori, Opt. Lett. **42**, 1512 (2017).
[16]Z. Tong and O. Korotkova, J. Opt. Soc. Am. A **29**, 2154 (2012).
[17]Y. Chen and Y. Cai, High Power Laser Sci. Eng. **4**, e20 (2016).
[18]Y. Gu and G. Gbur, Opt. Lett. **38**, 1395 (2013).
[19]X. Xiao and D. G. Voelz, Proc. SPIE **8874**, 887405 (2013).
[20]X. Xiao and D. G. Voelz, *Imaging and Applied Optics 2017 (3D, AIO, COSI, IS, MATH, pcAOP)*, PTu1D.3 (Optical Society of America, 2017).
[21]S. Cui, Z. Chen, L. Zhang, and J. Pu, Opt. Lett. **38**, 4821 (2013).
[22]M. W. Hyde, S. Bose-Pillai, D. G. Voelz, and X. Xiao, Phys. Rev. Appl. **6**, 064030 (2016).
[23]M. W. Hyde IV, S. Bose-Pillai, X. Xiao, and D. G. Voelz, J. Opt. **19**, 025601 (2017).
[24]M. W. Hyde and S. R. Bose-Pillai, Opt. Lett. **42**, 3084 (2017).
[25]E. Bolduc, N. Bent, E. Santamato, E. Karimi, and R. W. Boyd, Opt. Lett. **38**, 3546 (2013).
[26]M. W. Hyde, S. Basu, D. G. Voelz, and X. Xiao, J. Appl. Phys. **118**, 093102 (2015).
[27]C. Rosales-Guzmán and A. Forbes, *How to Shape Light with Spatial Light Modulators* (SPIE Press, 2017).
[28]J. W. Goodman, *Introduction to Fourier Optics*, 3rd ed. (Roberts & Company, 2005).
[29]D. G. Voelz and M. C. Roggemann, Appl. Opt. **48**, 6132 (2009).
[30]D. G. Voelz, *Computational Fourier Optics: A MATLAB Tutorial* (SPIE Press, Bellingham, WA, 2011).
[31]J. D. Schmidt, *Numerical Simulation of Optical Wave Propagation with Examples in MATLAB* (SPIE Press, Bellingham, WA, 2010).